An IoT-based GNSS platform for infrastructure monitoring

Raniero Beber [1], Luca Morelli [1], Fabio Remondino [1], Francisco Hernandez[2],

[1] 3D Optical Metrology (3DOM) unit, Bruno Kessler Foundation (FBK), Trento, Italy – Email: (rbeber, lmorelli, remondino)@fbk.eu

[2] Worldsensing, Barcelona, Spain – fhernandez@worldsensing.com

KEY WORDS: structural monitoring, continuous monitoring, LoRa, dam, tailing storage facilities, RTK, PPK, GNSS

ABSTRACT

In recent years, mining operators have adopted Information and Communications Technology (ICT) for monitoring and inspection operations but archaic/manual processes to collect and analyse data are still in use, thus making the protection of mining critical assets a costly and highly complex problem, reducing the capabilities of the monitoring system to trigger automatic alarms. Within the SEC4TD project, a low-cost IoT-based GNSS positioning device is developed, with the aim to provide accurate absolute positions of infrastructures. The solution includes the use of a two bands (L1, L2) GNSS receiver, long power autonomy and RTK correction on edge nodes. The paper describes the first prototype and the initial testing to evaluate its positional precision. A long term evaluation over 15 days is performed including a comparison with a high-end receiver. Lastly, field conditions are mimicked by reducing to 60 the number of epochs used in estimating the position each hour allowing for continuous monitoring of the infrastructure of interest.

1. INTRODUCTION

In the first two months of 2024, we witnessed two tragic large landslides happening at mining sites: 25th January mine waste failure in Myanmar[1], 13th February landslide at Çöpler Mine in Turkey[2]. Slope instability, earthquakes, overtopping, inadequate foundations and seepage are the most common reasons for tailings containment wall failures (Clarkson and Williams, 2020). Those events, like many others in the past years, remind us of the urgency and importance of accurate and continuous monitoring of mining sites. In recent years, mining operators have adopted Information and Communications Technology (ICT) but still use archaic/manual processes to collect and analyse data, thus making the protection of the mining critical assets a costly and highly complex problem, moreover reducing the capabilities of the monitoring system to trigger automatic alarms. In this context, Tailings Storage Facilities (TSFs) are one of the most sensitive physical assets to be secured to guarantee mines infrastructure safety. Historically, there are about 20 TSFs failures per decade (Walker, 2015) showing a tendency to shift these hazards from developed countries to developing countries and –in the last years– a few of them generated a tendency to mistrust the mining sector.

Pushed by these monitoring needs, the EIT-RM SEC4TD project (https://sec4td.fbk.eu/) aims to implement an innovative monitoring and responsive risk management system for TSFs based on the combination of three products: i) accurate absolute positioning solution supported by Internet of Things (IoT) technology, ii) real-time updating of deformations of the dam's structural and geotechnical model for early identification of critical and risky situations and iii) a portfolio of innovative applications to support decision-maker. This paper presents the development and analysis of the first product, i.e. the IoT-based GNSS solution. This solution needs for i) a simple deployment on site, ii) to scale easily due to the physical extend of the structure object to monitoring iii) to withstand the remote environment with low connectivity and at times harsh weather conditions. These requirements puzzled the industry for quite a while, we aim to bring a contribution to this via the proposed prototype.

2. RELATED WORKS

In Scaioni et al. (2018) techniques for dam deformation monitoring are compared and reviewed. Deformations in dams are typically monitored by measuring the displacement of a series of control points over time. These points are distributed along the crest, the base, and the sides of the dam to track both deformations and rigid body displacements, such as rotations. The most traditional method for achieving millimetric accuracy in the measurement of control points involves the use of geodetic networks. Standard practice includes employing a theodolite for planar deformations and an optical level for vertical deformations. However, these surveys are time-consuming and do not facilitate continuous monitoring. The introduction of robotic total stations has improved this limitation, enabling daily or more frequent measurements with automated targeting of control points. Despite these advancements, the use of such technology requires a clear line of sight and is affected by variable atmospheric refraction indices over long distances. Global Navigation Satellite System (GNSS) is a valid alternative to geodetic networks. GNSS is able to reach same level accuracies without the need of control points in line of sight. It requires specialized personnel only for design, installation and processing but not for data acquisitions (Reguzzoni et al., 2022). The use of automated GNSS for navigation, positioning and monitoring applications is increasingly present with a trend of integrating multi-frequency and multi-constellation receivers with camera sensors (Morelli et al., 2022; Oniga et al., 2024) and IoT systems for real-time data transmission and processing (Huang et al., 2023; Hamza et al., 2023; Xue et al., 2023). Real-time kinematic (RTK) solutions are preferred since they provide onsite positioning and in the cases of small baselines between base and rovers, as is the case for dam s and bridges monitoring, the atmospheric influence can be neglected (Xi et al., 2023).

In the literature different complementary IoT and GNSS solution are applied in a variety of fields. Vadlamudi et al. 2024, thanks to Adriano technology, deployed a dense sensor network out of small, single-recurrence GNSS receivers. They can monitor the overall electron concentration in the ionosphere in real-time. In order to monitor two active landslides, Lau et al. (2023) deployed MEMS accelerometers and GNSS receivers, combining the two data source the authors were able to see how and when the landslide is triggered by the rainfall. Similarly, Marino et al.,

[1] https://eos.org/thelandslideblog/myanmar-1

[2] https://eos.org/thelandslideblog/copler-mine-1

(2023) developed a low-cost IoT solution for hydrological monitoring of slopes on pyroclastic deposits. To ensure safety of the construction site environment and workers through the real-time monitoring, Ragnoli et al. (2022) connected IMU nodes with GNSS and RFID sensors via LoRa modulation technology.

3. DEVELOPED IoT-BASED GNSS SOLUTION

The functional requirements identified for monitoring TSF infrastructures include:

- Continuous operation during long periods (e.g. more than 2 years) without maintenance needs;
- Provide real-time and high-quality positional data;
- Alert when a malfunction of the sensors occurs or the acquired data present anomalies;
- Low power consumption;
- Bandwidth availability of the communications channel.

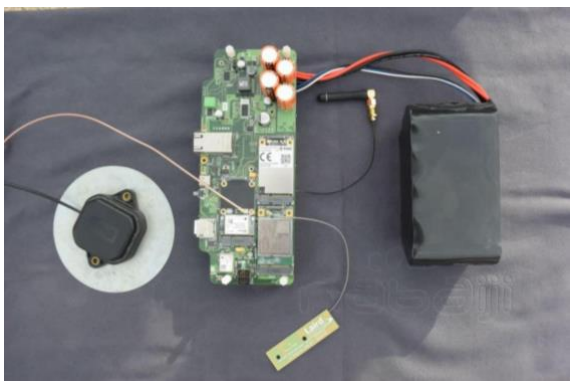

Figure 1: The initial set-up of the proposed IoT-based GNSS device: antenna (left), GNSS receiver node (middle), battery (right).

To achieve these requirements, a low-cost IoT-based GNSS node (Figure 1) was assembled in order to continuously monitor complex structures located in remote places. It is composed of:

- Multiband and multi-constellation GNSS system;
- A patch antenna;
- Low power GNSS receiver;
- Battery with a minimum lifetime of two years;
- Radio transceivers based on LoRa;
- TCP server for NMEA data transmission.

The node can function both as a rover and as a base, with multiple nodes communicating with the base station, which is positioned at a stable location near the dam and sends RTK corrections. The advantage of LoRa communication lies in long distance communication, low power consumption and high obstacle penetration (Yao et al., 2022). The selection of the antenna was based on the material, the energy consumption and the setup. An external, active, multiband antenna with a ground plane to maximize performance has been used. The antenna and the receiver are connected via a coaxial cable approximately ten centimetres in length to minimize signal attenuation.

The proposed IoT-based GNSS device can operate in Real-Time Kinematic (RTK) or Post-Processed Kinematic (PPK). PPK allows post-processing of GNSS RAW data while RTK processes GNSS data on the IoT device (after having received the correction information) and sends back the processed GNSS data. The main bottleneck for RTK is sending the GNSS correction data so that each of the nodes can process the GNSS raw satellite data on to provide back corrected GNSS positioning data. Therefore, the entire correction transmission process has been optimized to minimize battery consumption. As visible in Figure 2, multiple rovers can receive corrections from a single base, which transmits the necessary data for RTK solution via LoRa communication. This enables precise positioning data. After performing RTK calculations, the rovers send sensor data and statistics through the gateway via LoRa. Additionally, the device can be remotely configured through the gateway using LoRa communications.

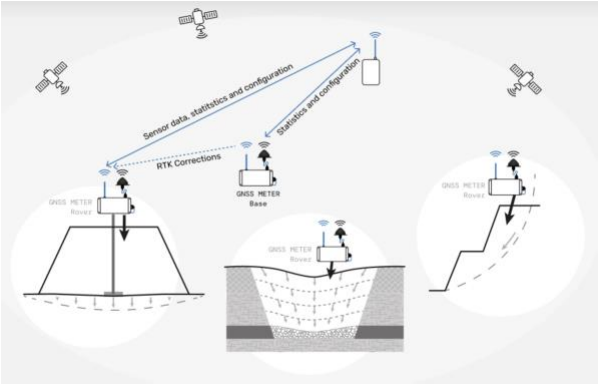

Figure 2: IoT solution setup for field deployment (Worldsensing, 2024).

The presented prototype of the SEC4TD project aims at providing an easy to deploy and scalable node able to monitor displacements of large infrastructures with a low level of maintenance. In this fashion a previous work for landslide monitoring has been presented by Zuliani et al. (2022). The main difference between their approach and our solution is the use of a two bands (L1, L2) GNSS receiver, the power autonomy and RTK correction on edge nodes.

4. INITIAL TESTING AND VALIDATION

To test the proposed solution, a series of IoT GNSS nodes were deployed to evaluate the GNSS RTK performance conditioned on several variables, utilizing a reliable and low-latency wireless communication link between the base and the rover. This performance serves as the baseline, with the primary objective being to understand the performance of RTK technology, without considering the potential degradation induced by a low-bandwidth radio channel.

In Figure 3 two independent experiments are reported, and it includes a scatter plot of the relative error for single samples (one sample per navigation epoch computed every second), followed by a box plot of the error. In this context, the error is defined as the Euclidean distance to a known geodetic point. The rover, positioned in the geodetic point, was separated from the base by 1.34 km. Each experiment lasted for about 14 hours, with colours representing different hours. The minimum observed CEP is around 0.5 cm with maximum error up to 2.5 cm. It is important to note that these results should be treated as a lower bound on accuracy. The CEP is defined as the radius of a circle centred at the mean point, with a 50% probability of a hit (indicating that half of the samples are inside the radius defined by the CEP). In Figure 3a-b two independent experiments are reported, and it includes a scatter plot of the relative error for single samples (one sample per navigation epoch computed every second), followed by a box plot of the error. In this context, the error is defined as the Euclidean distance to a known geodetic point. The rover, positioned in the geodetic point, was separated from the base by 1.34 km.

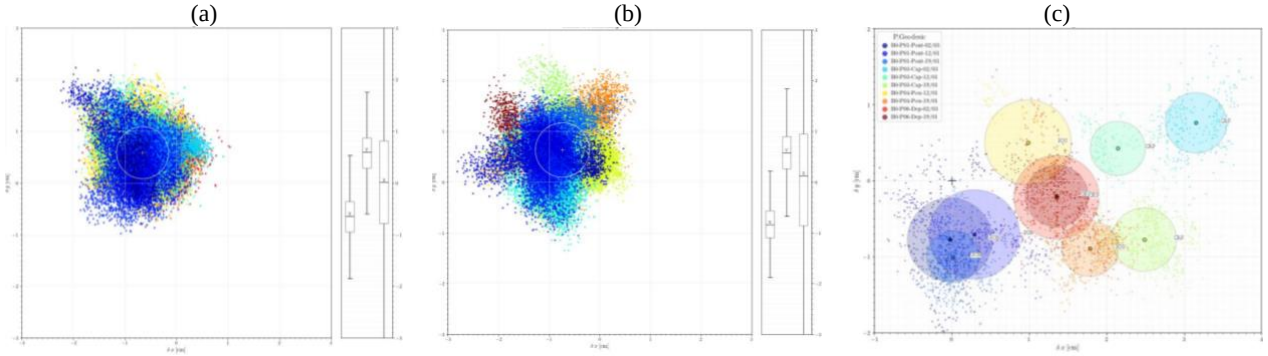

Figure 3: Relative positioning error (the different colours represent one hour of consecutive solutions) for two tests with Circular Error Probable (CEP): CEP = 0.504 (a) and CEP = 0.535 (b). Absolute displacement error of measurements (c).

Each experiment lasted for about 14 hours, with colours representing different hours. The minimum observed CEP is around 0.5 cm with maximum error up to 2.5 cm. It is important to note that these results should be treated as a lower bound on accuracy. The CEP is defined as the radius of a circle centred at the mean point, with a 50% probability of a hit (indicating that half of the samples are inside the radius defined by the CEP).
Figure 3c shows a positioning error for three different rover-base distances with a 20% degradation in the CEP when is 5 km compared to the optimal conditions test measured at 1.3 km. This suggests that signal variance increases with distance, but not excessively. The experiments were done in three different days for two locations: Pont (600 m distance) and Capitolio (5 km), while on two different days for Pou (5.5 km) and Depuradora (1.5 km). Circles represent the relative error median, and the circle marker indicates the mean of each experiment. For small rover-base distances, (Pont and Depuradora) are much closer than those from large distances. This suggests that small sample sizes (of a few minutes) may be sufficient to estimate the mean (in this case, an error of around 1 cm, which is less than the error reported by the IGCG - responsible for the geodetic points in Catalonia, Spain). However, this is not the case for far distances like Pou and Capitolio, where samples taken on different days diverge, and the errors variance, although within the same day, is similar.

5. LONG TERM TESTING

To further test and validate the new GNSS-IoT based node long acquisitions were performed. From the 13th of January 2024 to 29th of the same month, the rover was configured to use 3 constellations (GPS, GLONASS, GALILEO). RTK corrections were sent from a base with the same configuration, located 450m from the rover. The rover was operating in series of 30min, e.g. every 30min a COLD start reset was sent erasing ephemerides and almanacs databases so it was starting without any previous knowledge of satellite orbits. When switched on again, the base receiver collects the new navigational data and after a few seconds is able to send RTK corrections to the rovers. This operation continues until the next restart. In the absence of RTK corrections due to a temporary deficiency in the network connection, the rover estimated the position in single point positioning mode.
The full solution is aggregated daily by the median value and Figure 4 shows the trend of X and Y coordinates with respect to a fiducial point of known coordinates (centimetre precision). The mean deviation from the ground truth position is of 17 mm on the plane with a standard deviation of 4 mm (Table 1).
The RTK solution is also plotted against the fiducial point coordinate: in Figure 5a and Figure 5b the time series of RTK solutions computed during the 16 days of acquisition for X (East) and Y (North) are reported, respectively clustered per acquisition day. To better appreciate the distribution of the solution, violin plots are reported in Figure 6 with markers at 1, 25, 50, 75, 99 quantiles and coordinates plotted on each of the rows.

Coordinates	Mean μ [mm]	Standard deviation σ [mm]	Range r [mm]
X	9.9	3.9	11.9
Y	13.8	0.9	3.3
XY	17.0	4.0	12.3

Table 1: Metrics for the IoT-based GNSS node used as rover.

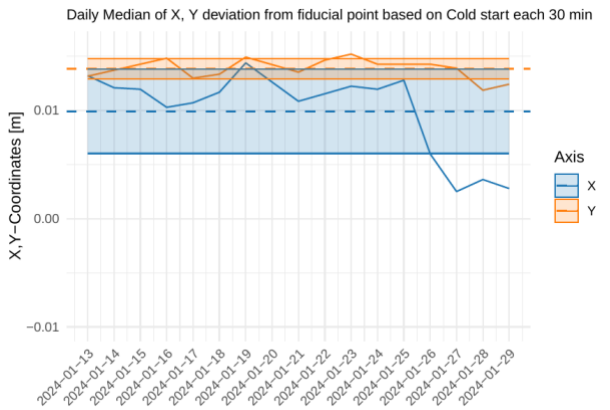

Figure 4: Long term test of IoT-based GNSS node. Daily median for X and Y direction are reported. Mean and standard deviation of the daily median are also shown.

6. PRECISION COMPARISON WITH HIGH-END GNSS RECEIVER

To understand the node precision in the context of well-established GNSS practice, a high-end GNSS receiver, namely a Topcon AGM-1[3], was used to acquire for a period of 15 days. The Topcon base and rover were positioned on two fiducial points of known coordinates. PPK processing was adopted to converge to solution based on 6h or 1h acquisition windows.

[3] https://mytopcon.topconpositioning.com/na/agriculture-gnss-and-guidance/gnss-receivers-and-controllers/agm-1

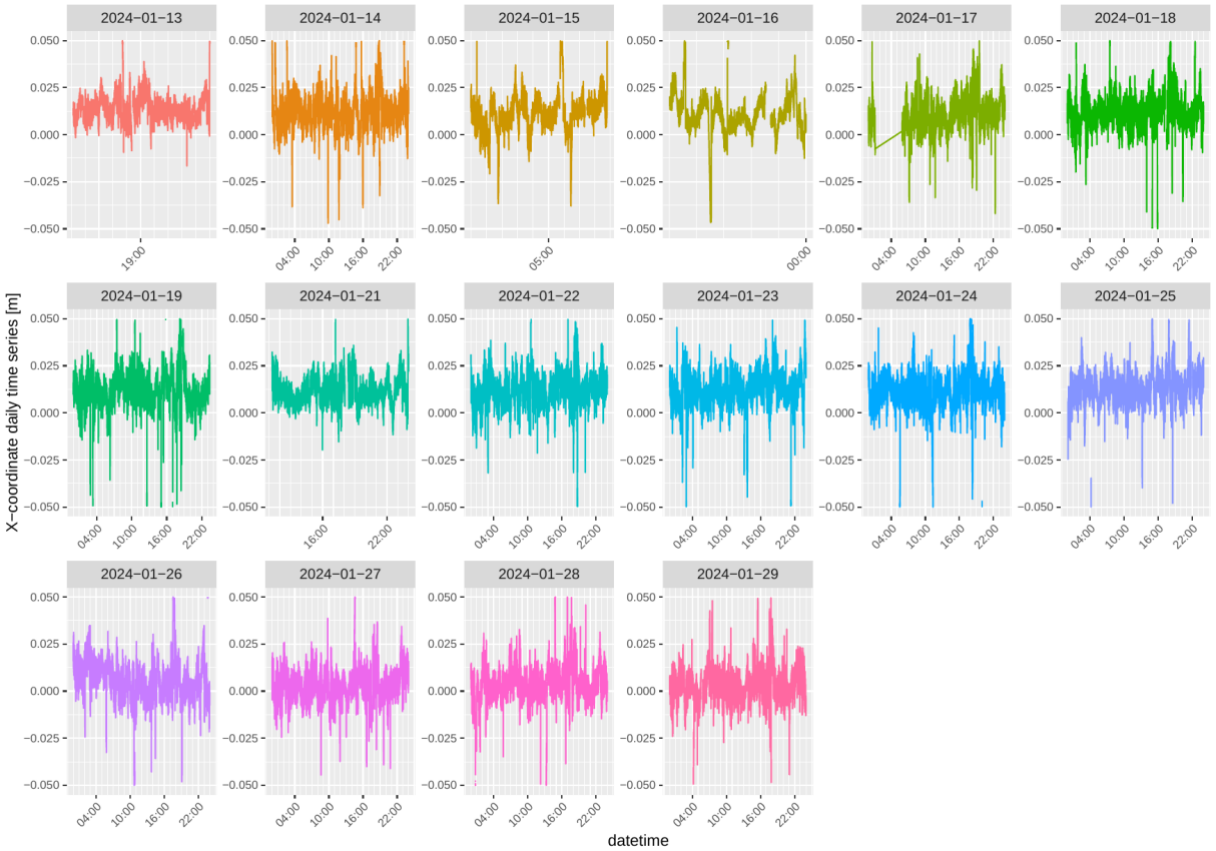

(a)

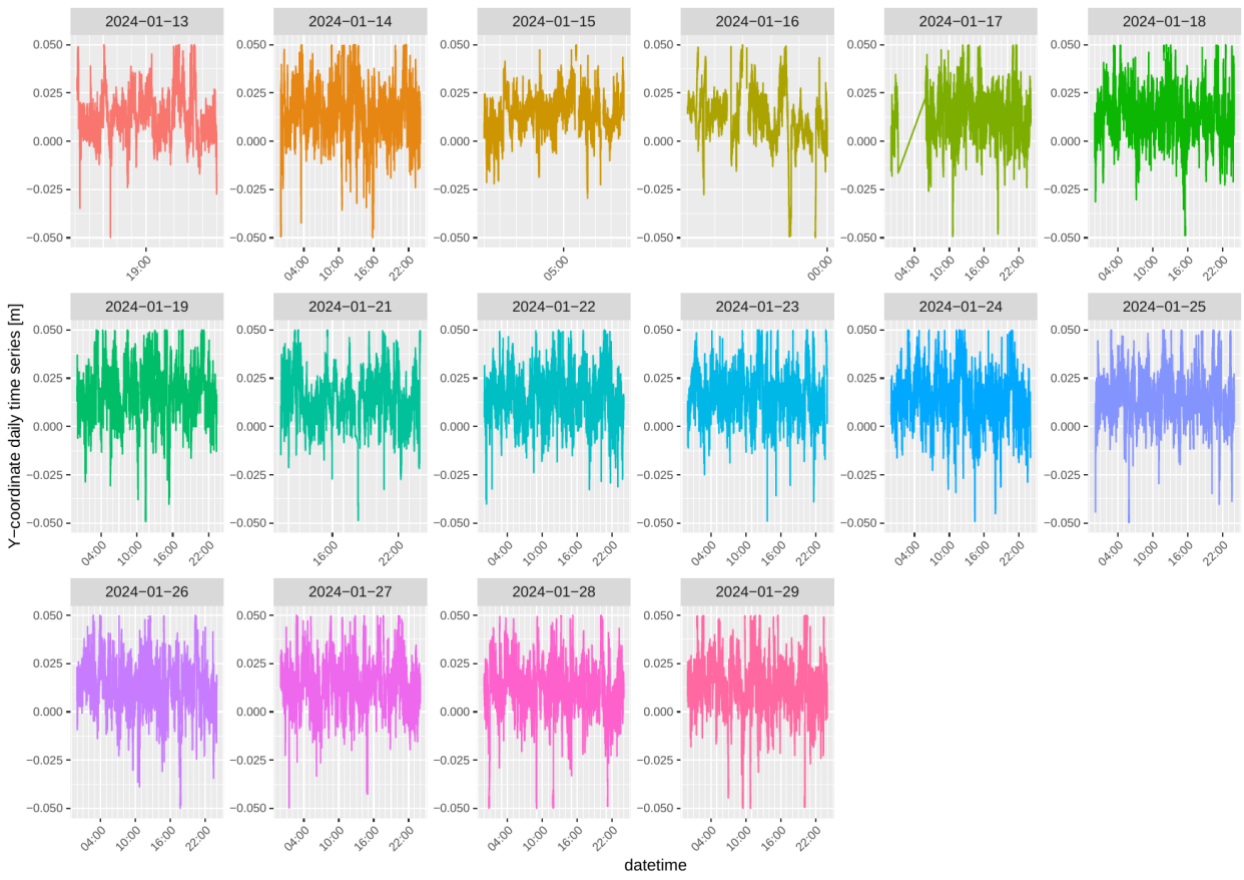

(b)

Figure 5: Long term testing of IoT based GNSS node as RTK rover. The time series of RTK positioning solutions are computed during the 16 days of acquisition and reported for X (a) and Y (b).

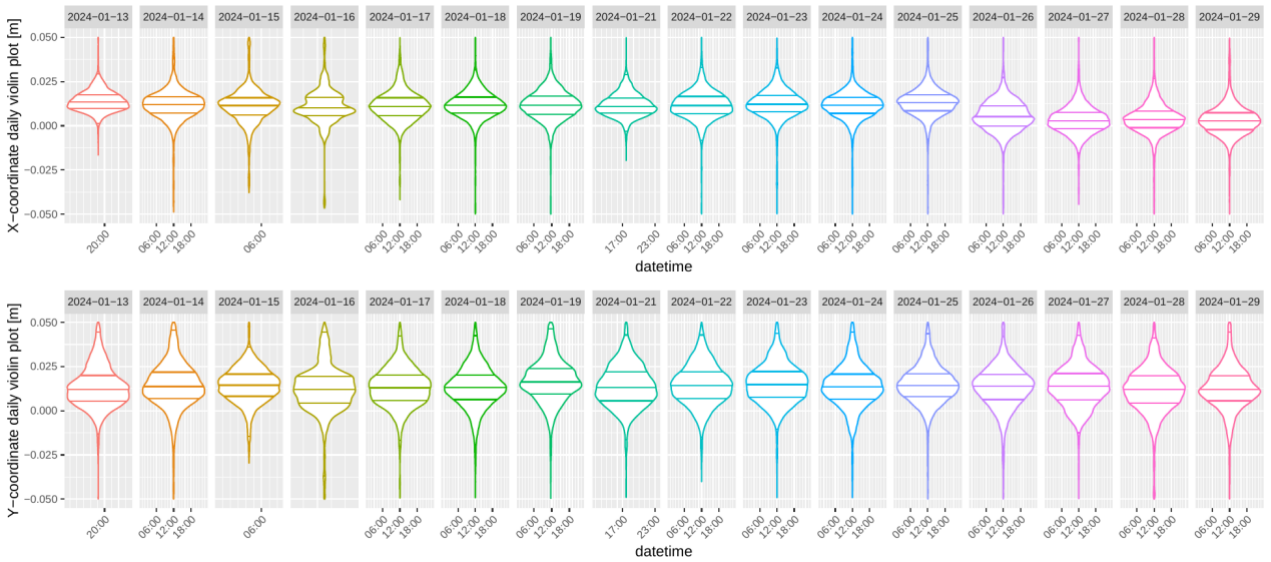

Figure 6: Long term testing of IoT-based GNSS node as RTK rover. The time violin plot of RTK positioning solutions is computed on the 16 days of acquisition and reported for X and Y. The violin plot reports 1, 25, 50, 75, 99 quantiles and are calculated per day.

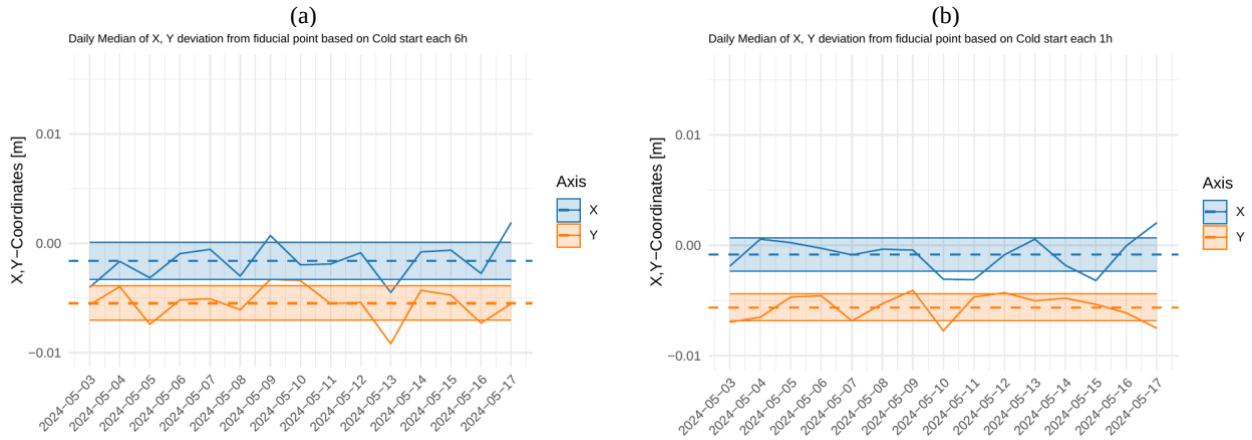

Figure 7: (a)Topcon PPK solution using 6h windows; (b)Topcon PPK solution using 1h window

	6h acquisition			1h acquisition		
	μ [mm]	σ [mm]	r [mm]	μ [mm]	σ [mm]	r [mm]
X	-1.6	1.7	6.4	-0.8	1.5	5.3
Y	-5.5	1.6	5.9	-5.6	1.2	3.7
XY	5.7	2.3	8.7	5.7	2.0	6.4

Table *1*: Accuracy and precision of high-end GNSS receiver.

The data processing was performed with RTKLIB 2.4.3 (Takasu, 2013), and the resulting accuracy and precision are reported in Table 2. Figure 7a report the best precision achievable by the high-end device based on PPK solution on 6h long acquisition. If the acquisition window is shortened to 1h the solution stability is guarantee as visible in Figure 7b. This becomes particularly significant since shorted acquisition windows would allow a more continuous monitoring of the infrastructure of interest. In Table 2 the overall mean, standard deviation and range over the 15 days acquisition period at the two different processing windows are reported.

7. PRECISION IN SIMULATED FIELD DEPLOYMENT

As introduced in the beginning, being able to perform continuous monitoring of critical infrastructures in a remote environment is paramount. More frequent acquisition allows a close monitoring and early detection of anomalies in the response of the structure to external forcing. To mimic the actual deployment of the IoT device in the field, thus saving battery and extend its life-span, the RTK solution has been downgraded to take advantage of only 60 acquisitions after the first cold start for each hour. This is comparable to the site deployment where the device remains in sleep mode until is waken up for 60 seconds acquisition period each hour. Similarly, the high-end receiver RAW data have been processed in PPK just for 60 acquisitions for each hour. The results of this comparison are reported in Table 3 and Figure 8.

	IoT node RTK			Topcon PPK		
[mm]	μ	σ	r	μ	σ	r
X	9.8	4.9	14.0	-0.2	2.3	7.3
Y	13.2	1.8	5.9	-4.6	1.8	6.7
XY	16.5	5.2	15.2	4.6	3.0	9.9

Table 2. Comparison of IoT node in RTK and High-end receiver PPK for 60 acquisitions each hour.

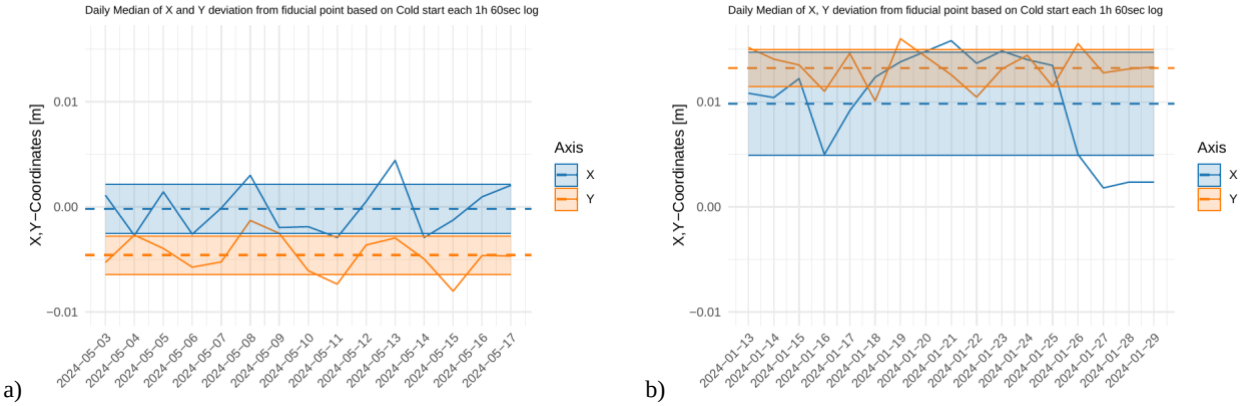

a) b)

Figure 8: (a) Topcon PPK solution using 60 second data each hour after a COLD start (b) IoT-based GNSS RTK solution using 60 second data each hour after a COLD start.

Thanks to the high quality of the antenna and receiver of the high-end device, Figure 8a set the baseline for the precision comparison. The PPK solution with 60 observations each hour (mediated daily) is constrained to a range of 7.3 and 6.7 mm for X, Y respectively during a period of 15 days. The IoT-based GNSS node perform reasonably well in this comparison (Figure 8b) with a range of 14 and 5.9 mm in X and Y. Given the advantage in battery life that such operational solution would provide the loss in precision is reasonably well accepted for the TSF monitoring purpose.

8. CONCLUSIONS

We have presented a low-cost GNSS-IoT prototype which is under development, testing and validation in controlled environments. The product is set to be delivered to the end users by the end of 2024. A compact prototype is under finalisation for dispatch to the SEC4TD case studies, in Poland (KGHM CUP) and Bosnia and Herzegovina (ArcelorMittal).
Results shows that the prototype performed well both in continuous and start-and-stop mode over the 15 days of acquisitions. In the first scenario, with a cold start every 30 minutes, the systems achieved an accuracy of 17 mm in the plane with a standard deviation of 4 mm within a range of 12 mm. In the simulated field working mode, reducing the RTK solution to 60 epochs, lead to similar accuracy increasing the standard deviation to 5 mm and consequently the range to 15 mm. Further testing and validation are foreseen on the data acquired on the two pilot sites of the project.

ACKNOWLEDGMENTS

The project activities have been supported by the EIT-RM project SEC4TD - Securing tailings dam infrastructure with an innovative monitoring system (https://sec4td.fbk.eu/).

REFERENCES

Clarkson, L. and Williams, D., 2020. Critical review of tailings dam monitoring best practice. *International Journal of Mining, Reclamation and Environment*, 34(2), pp.119-148.

Hamza, V., Stopar, B., Sterle, O. and Pavlovčič-Prešeren, P., 2023. A cost-effective GNSS solution for continuous monitoring of landslides. *Remote Sensing*, 15(9), p.2287.

Huang, G., Du, S. and Wang, D., 2023. GNSS techniques for real-time monitoring of landslides: A review. *Satellite Navigation*, 4(1), p.5.

Yao, F., Ding, Y., Hong, S. and Yang, S.H., 2022. A survey on evolved LoRa-based communication technologies for emerging internet of things applications. *International Journal of Network Dynamics and Intelligence*, pp.4-19.

Lau, Y.M., Wang, K.L., Wang, Y.H., Yiu, W.H., Ooi, G.H., Tan, P.S., Wu, J., Leung, M.L., Lui, H.L. and Chen, C.W., 2023. Monitoring of rainfall-induced landslides at Songmao and Lushan, Taiwan, using IoT and big data-based monitoring system. *Landslides*, 20(2), pp. 271-296.

Marino, P., Roman Quintero, D.C., Santonastaso, G.F., Greco, R., 2023. Prototype of an IoT-based low-cost sensor network for the hydrological monitoring of landslide-prone areas. *Sensors*, 23(4), p.2299.

Morelli, L., Menna, F., Vitti, A. and Remondino, F., 2022. Action Cams and Low-Cost Multi-Frequency Antennas for GNSS Assisted Photogrammetric Applications Without Ground Control Points. *Int. Arch. Photogramm. Remote Sens. Spatial Inf. Sci.*, XLVIII-2/W1-2022, pp.171-176.

Oniga, E., Boroianu, B., Morelli, L., Remondino, F., and Macovei, M., 2024. Beyond ground control points: cost-effective 3D building reconstruction through gnss-integrated photogrammetry. *Int. Arch. Photogramm. Remote Sens. Spatial Inf. Sci.*, XLVIII-2/W4-2024, 333–339.

Ragnoli, M., Colaiuda, D., Leoni, A., Ferri, G., Barile, G., Rotilio, M., Laurini, E., De Berardinis, P. and Stornelli, V., 2022. A LoRaWAN multi-technological architecture for construction site monitoring. *Sensors*, 22(22), p.8685.

Reguzzoni, M., Rossi, L., De Gaetani, C.I., Caldera, S., Barzaghi, R., 2022. GNSS-based dam monitoring: The application of a statistical approach for time series analysis to a case study. *Applied Sciences*, *12*(19), p.9981.

Scaioni, M., Marsella, M., Crosetto, M., Tornatore, V. and Wang, J., 2018. Geodetic and remote-sensing sensors for dam deformation monitoring. *Sensors*, *18*(11), p.3682.

Takasu, T., 2013. Rtklib. Available: http:\\www. rtklib. com.

Vadlamudi, M.N., Jayanthi, N., Swetha, G., Nishitha, P., Al-Salman, G.A. and Saikumar, K., 2024. IoT Empowered GNSS Tracking in Real-time via Cloud Infrastructure. *Proc. IEEE 9th Int. Conference for Convergence in Technology*, pp. 1-6.

Xi, R., Jiang, W., Xuan, W., Xu, D., Yang, J., He, L. and Ma, J., 2023. Performance Assessment of Structural Monitoring of a Dedicated High-Speed Railway Bridge Using a Moving-Base RTK-GNSS Method. *Remote Sensing*, 15(12), p.3132.

Xue, C., Psimoulis, P., Horsfall, A., Zhang, Q. and Meng, X., 2023. Assessment of the accuracy of low-cost multi-GNSS receivers in monitoring dynamic response of structures. *Applied Geomatics*, 15(2), pp.315-326.

Walker, S., 2015. Tailings management strategies to meet today's demands. *Engineering and Mining Journal*, 216(11), p.44.

Worldsensing, 2024. https://www.worldsensing.com/

Zuliani, D., Tunini, L., Di Traglia, F., Chersich, M. and Curone, D., 2022. Cost-effective, single-frequency GPS network as a tool for landslide monitoring. *Sensors*, 22(9), p.3526.